*RevMexAA (Serie de Conferencias)*, **36**, 193–199 (2009)

# ASTROPHYSICAL JETS AS HYPERSONIC BUCKSHOT: LABORATORY EXPERIMENTS AND SIMULATIONS

A. Frank,[1] A. Ciardi,[2] K. Yirak,[1] and S. Lebedev[3]



RESUMEN

Los jets Herbig-Haro (HH) normalmente son interpretados como haces homogéneos de plasma viajando a velocidades hipersónicas. Las estructuras en los jets frecuentemente son atribuidas a variaciones periódicas o "pulsadas" en las condiciones de eyección. En esta contribución ofrecemos una alternativa a los modelos "pulsados" de jets protoestelares. Usando simulaciones numéricas directas y experimentos de laboratorio exploramos la posibilidad que los jets sean cadenas de nudos sub-radiales que se propagan en un medio inter-nudo. Nuestras simulaciones exploran una idealización de esta situación, inyectando esferas pequeñas ($r < r_{\rm jet}$) y densas ($\rho > \rho_{\rm jet}$) embebidas en un flujo homogéneo. Las esferas están inicializadas con velocidades que difieren por $\sim 15\%$ del flujo inter-nudo. Encontramos que el cambio de un flujo homogéneo a uno heterogéneo tiene consecuencias significativas, dado que los nudos densos interactúan entre ellos y con el medio inter-nudo de maneras diversas. También presentamos nuevos experimentos que, por primera vez, simulan aspectos de jets astrofísicos magnetizados. Nuestros experimentos exploran la propagación y la estabilidad de burbujas con jets internos super-magnetosónicos, radiativos y magnéticamente dominados. Los resultados son escalables a medios astrofísicos como resultado de la similaridad de los parámetros adimensionales que controlan los flujos en los dos ambientes. Estos experimentos muestran que los jets están sujetos a inestabilidades helicoidales que rápidamente fragmentan al jet para formar finas cadenas de nudos hipersónicos, proveyendo un posible fundamento para el modelo de "jet heterogéneo".

ABSTRACT

Herbig-Haro (HH) jets are commonly thought of as homogeneous beams of plasma traveling at hypersonic velocities. Structure within jet beams is often attributed to periodic or "pulsed" variations of conditions at the jet source. In this contribution we offer an alternative to "pulsed" models of protostellar jets. Using direct numerical simulations and laboratory experiments we explore the possibility that jets are chains of sub-radial clumps propagating through a moving inter-clump medium. Our simulations explore an idealization of this scenario by injecting small ($r < r_{\rm jet}$), dense ($\rho > \rho_{\rm jet}$) spheres embedded in an otherwise smooth inter-clump jet flow. The spheres are initialized with velocities differing from the jet velocity by $\sim 15\%$. We find the consequences of shifting from homogeneous to heterogeneous flows are significant as clumps interact with each other and with the inter-clump medium in a variety of ways. We also present new experiments that, for the first time, directly address issues of magnetized astrophysical jets. Our experiments explore the propagation and stability of super-magnetosonic, radiatively cooled, and magnetically dominated bubbles with internal, narrow jets. The results are scalable to astrophysical environments via the similarity of dimensionless numbers controlling the dynamics in both settings. These experiments show the jets are subject to kink mode instabilities which quickly fragment the jet into narrow chains of hypersonic knots, providing support for the "clumpy jet" paradigm.

*Key Words:* ISM: jets and outflows — stars: mass loss — stars: pre-main sequence

## 1. INTRO

Herbig-Haro objects have been the subject of significant analytical, observational, and numerical attention since their discovery. Observations using optical and IR techniques reveal that these jets typically show striking large scale collimation extending out to parsec distances combined with features appearing on a range of smaller scales. The nature of these jets as collimated mass loss from a central accreting source has been confirmed in numerous investigations. What remains unclear, however, is the exact mechanisms by which this mass loss is driven

[1]Department of Physics and Astronomy, University of Rochester, Rochester NY 14627, USA (afrank@pas.rochester.edu).
[2]LUTH, Observatoire de Paris et UMR 8102 du CNRS, 92195 Meudon, France.
[3]The Blackett Laboratory, Imperial College, London SW7 2BW, UK.

and the dynamics of the outflow during, and after the its launch. While the small scale features in the jets have been seen as interesting in their own right, in this contribution we argue that they may hold keys to understanding fundamental questions related to collimated outflows

The origin of "knots" and "clumps" in jets remains a subject of debate. Early studies focused on clumpyness of the HH bow shocks; Norman & Silk (1979) postulated the existence of single "interstellar bullets". Stationary crossing shocks due to an overpressured jet beam expanding and then recollimating were an early possibility that was considered for knots along the beam (Raga et al. 1990). More recently, Rubini et al. (2007) have suggested oblique shock focusing as a natural mechanism for hydrodynamic knot formation, though the presence of magnetic fields (Hartigan et al. 2007), precession (Masciadri et al. 2002), and interactions with the environment (Raga et al. 2002; de Gouveia Dal Pino 1999; Yirak et al. 2008) all offer other means by which dense clumps might be created. While considerable work has gone into these scenarios, currently the most favored model for the knots are internal working surfaces where shocks are driven down the beam by pulsation at the jet source. This "pulsation" model has been extensively explored by Raga and collaborators (Raga & Noriega-Crespo 1992; Biro & Raga 1994; Raga & Biro 1993). In pulsed jet simulations the density and velocity cross-sectional profiles $\rho_j(r)$ & $v_j(r)$ in the jet-launching region are kept fixed, while the magnitude of the velocity varies sinusoidally. The pulsation scenario has become so dominant that even when attempting to address questions unrelated to clump formation, periodic inflow variations are frequently employed.

A variety of observational signatures can be recovered via pulsed jet models through careful choice of specific jet physical parameters and sinusoidal variability. In Raga et al. (2002) a two-mode launching model was proposed using velocity histories extracted from observations of HH 34 and HH 111. Using these pulsation modes, axisymmetric hydrodynamic simulations provided a convincing match to the location of the leading bow shock and the location of bright knots in the beam. These results provide strong support for pulsed jet models.

A detailed examination of jets observed at the highest spatial resolution, however, show features which do not fit into the pulsed jet paradigm. In particular, a number of "archetypal" jets show features at scales below the jet radius ($r < r_j$) which are distinctly displaced from the jet axis. In the case of HH 47, the jet clearly shows a non-axisymmetric morphology in the form an apparent helical bending of the beam (Hartigan et al. 2005). The beam itself is defined by a sequence of quasi-periodic knots with displacements to either side of the nominal jet axis. Explanations for this bending have included impacts with objects (Raga et al. 2002; de Gouveia Dal Pino 1999), magnetic fields (Hartigan et al. 2007) and precession of the jet source (Masciadri et al. 2002). In this contribution we consider the presence of subradial, non-axisymmetric features to be a challenge to the pulsed jet paradigm. We consider an alternative to the pulsed jet model and investigate the consequences of intrinsic density heterogeneity in jet formation and evolution (Yirak et al. 2009).

We are motivated to explore this model by both observations and new, high energy density laboratory astrophysics (HEDLA) plasma experiments. The second half of this contribution discusses those experiments. Using pulsed power, wire array technologies (Lebedev et al. 2004, 2005; Ciardi et al. 2007) have presented experiments that track the evolution of fully magnetized, hypersonic, radiative jets. The stability of hydro and MHD jets has long been a topic of debate and these experiments shed some light on the real dynamics of 3D systems. The experiments show that kink mode instabilities strongly affect the jet. As the kink mode grows into the non-linear regime it disrupts but does not destroy the jet. The saturation of the instability transforms the jet into a sequence of collimated chains of knots which propagate with a range of velocities. These experiments represent the first time the fully multidimensional time-dependent dynamics of radiative magnetized jets have been observed. We note that numerical simulations of these processes are necessarily limited in resolution and are subject to questions of numerical boundary conditions, an issue not affecting the experiments.

Thus, we propose a new model in which jets are essentially heterogeneous chains of bullets. As we shall see, the consequences of this model lead to important insights about the dynamics of jets after their launching.

### 1.1. *Simulations*

Numerical simulations of our model were undertaken with the *AstroBEAR* computational code (Cunningham et al. 2009) Information about the *AstroBEAR* code may be found online, at `http://www.pas.rochester.edu/~bearclaw`. Here, the code solved the 3D hyperbolic system of equations for inviscid, compressible flow using a spatial second-order and temporal first-order accurate MUSCL

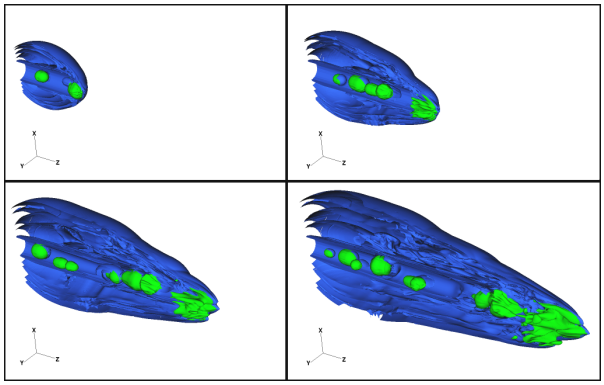

Fig. 1. Isocontours of logarithmic density at four times in the simulation, $t$ =30, 53, 77, and 100 yr. The clumps are depicted in light green, with the jet material in blue. The $yz$-plane along the jet axis clips the jet material contours.

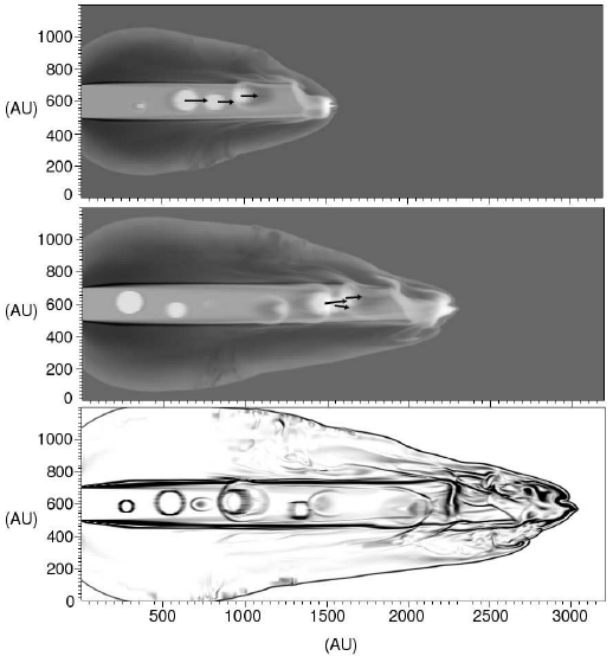


Fig. 2. The top two panels give grayscale images of logarithmic density in the $yz$-plane on the jet axis at two different times, $t$ =53 and 77 yr, corresponding to the lower left and upper right panels of Figure 1. Lighter gray corresponds to denser material. Velocity vectors originating at three knots have been overlaid, and they are seen to change as the knots interact. The bottom panel shows a synthetic Schlieren image at $t$ = 100 yr, which illuminates such features as a clump with a forward bow shock at $z$ =2100 AU, a clump with reverse bow shock at $z$ =900 AU, and clump-induced "spur shocks" at several places along the jet beam. The disk-like feature at $z$ = 2300 AU is discussed further in the text.

scheme using a Roe-averaged linearized Riemann solver. Simple radiative cooling is included separately using an iterative source term with a cooling curve.

The inhomogeneities in the beam were introduced as spherical density and velocity perturbations in an otherwise smooth beam: we shall refer to the former as "clumps" and the latter as the "jet." We begin with a Mach 30, over-dense ($\chi_{ja} \equiv \rho_j/\rho_a = 10$), and overpressured ($p_j/p_a = 10$) jet. The clumps all had the same initial number density of $\rho_c$=$10^3$ cm$^{-3}$, yielding density ratios of $\chi_{cj} \equiv \rho_c/\rho_j$=10 and $\chi_{ca} \equiv \rho_c/\rho_a$=100. The clumps were seeded with radii and velocities that were random. The $y$- and $z$-locations of the clumps in the jet were random with the constraint that the entire clump be located within the jet beam. At the maximum AMR level, the jet radius was resolved by 24 cells, and the clump radii by 6–14 cells.

A time-sequence of the simulation is given over four panels in Figure 1. Density plots and a Schlieren image are shown in Figure 2. Figure 1 shows a 3D representation of the simulation in the form of a set of iso-density contours. In the panels, the jet beam enters from the left hand side of the grid and propagates to the right. Shortly after the start of the jet, knots appear with random sizes, locations, and speeds. The figure has been adjusted to track the evolution of the clumps via an iso-density contour of a passive clump tracer (in green). Thus the clumps are readily recognizable as initially spherical inclusions within the beam close to the inflow boundary cells. As the simulation progresses, the clumps evolve via their interaction with the inter-clump material in the beam and, in some cases, with other clumps.

Once clumps are launched into the jet there are three possible consequences. The first consequence is the clump propagating downstream unimpeded and colliding with the jet head. In this case the dense clump may break through the bow shock defining the front edge of the jet leading to significant non-axisymmetric structures there. This behavior is apparent in both Figures 1 and 2, where a dense clump has already traversed the jet length and propagated through the jet shock/bow shock structure at the terminus of the beam. The presence of a significant "knob" protruding at the lower edge of the jet head defines the extent of the clump which now forms the leading edge of the jet. A second possibility, however, is that the clump will not make it to the leading edge of the jet. A clump compressed

by a strong transmitted shock wave (in this case the transmitted wave originates from its relative motion within the beam) will eventually be destroyed in a "cloud crushing time" given approximately by $t_{cc} = 2r_c\chi_{cj}^{1/2}/|\Delta v_c|$ where $\chi_{cj} = \rho_c/\rho_j$. If this happens before the clump reaches the jet head then the clump material will be dispersed within the beam.

The third possibility for the long term evolution of a clump is interaction with another clump. The interaction can take the form of direct or glancing collision depending on the impact parameter $b$. Even when $b > 2r_c$ there can still be interactions between a clump-driven bow shock and a neighboring clump. Figures 1 and 2 show a number of such interactions occurring. By the last panel of Figure 1, clump collisions have resulted in a merged structure near the head of the jet, and their effect on each other and on the jet beam itself is complex. It is noteworthy that the collision, compression and subsequent merger of clumps can come to resemble the internal working surfaces in homogeneous, pulsed jets. The difference between homogeneity and heterogeneity is particularly striking for glancing clump collisions: $0 < b < 2r_c$. In these cases the clump-clump interaction will be off center and one can expect from momentum conservation that non-axial mot ions will result. Figure 2 illustrates this point showing the off-center collision of three clumps. Before the collision the velocity vectors of all three clumps are purely axial $\vec{v} = v_z\hat{e}_z$. After the collision the clumps have acquired transverse $v_r$ velocities. The ability to generate non-axial motions within the beam via clump interactions is an important point as proper motion studies of highly resolved HH jets show knot to knot variability in both direction and speed.

In many studies, lifetimes of features along an HH jet beam are derived by relating the current position of the feature and its proper motion. Full velocity histories of jets have been derived in this way from observations in terms of multiple pulsation modes at the jet launch region. Our models shed new light on the issue of recovering pulsation histories from observations. We find that assuming periodic injection histories can bias the description of jets. For each data frame in our simulation we attempted to reconstruct a periodic inflow history based on the location of knots in the beam. In Figure 3, the axial density profile is given in the left panel with knots identified by circles. We then take the velocities at these positions to be the knot velocities. We found that at each time we were able to get good fits to a periodic ejection even though no such history was imposed on the jet. The three panels of Figure 3 show the result of

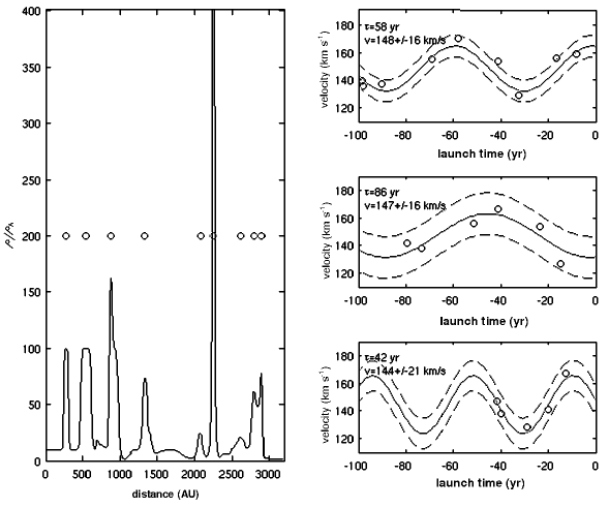


Fig. 3. Left: The axial density profile normalized by the ambient density, $\rho/\rho_a$, is plotted with positions designated as "knots" given by "○". Right: From top to bottom, velocities for knots ("○") versus their launching (dynamical) time at $t$ =100, 80, and 40 yr. Results from least-squares fits are shown with 1-$\sigma$ error overlaid. The period $\tau$ and mean velocity with single-mode sinusoidal amplitude, $v_j = v_{j,0} \pm v_j^{(1)}$, are printed on each panel.

least-squares fits to the data at different times with 1-$\sigma$ error bounds overlaid. The average velocity of the knots remains roughly constant for each of these three times and is close to the jet velocity ($v_j = 150$ km s$^{-1}$), as expected. However, the amplitude of the determined period varies by $\sim 30\%$ over time, and the period itself varies by over 100%. The goodness of the fits, though less at $t = 80$ yr than the other two times depicted, appears adequate. Although not explicitly shown here, variation in the fit results is correlated with knot-knot interactions. Thus, determination of periodic velocity histories from proper motions must be considered suspect.

### 1.2. *Laboratory Experiments*

Our High Energy Density Experiments were carried out at the MAGPIE pulsed-power facility at Imperial College, which delivers a peak current of 1 MA with a rise time of 240 ns. The experimental load consists of a flat 6 or 6.5 $\mu$m thick Aluminium foil connecting two cylindrical, co-axial electrodes. The associated numerical simulations are performed with our 3D, resistive MHD code GORGON. Further details of the experimental facility, the experimental set-up including the diagnostics used, and the MHD code can be found in Lebedev et al. (2005) and Ciardi et al. (2007). A schematic diagram of the evolution

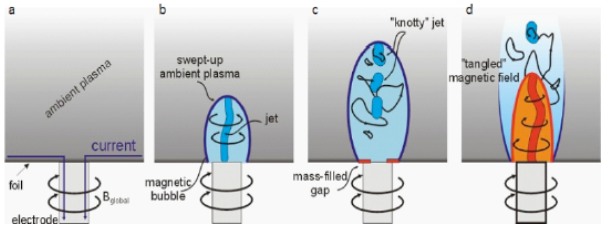


Fig. 4. Schematic of the evolution of a jet/bubble system.

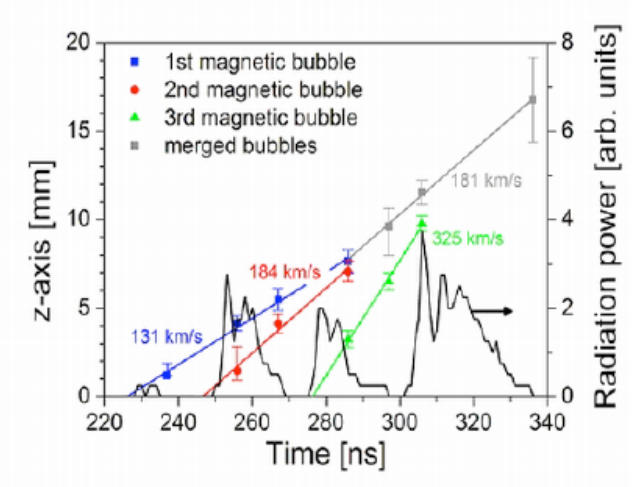


Fig. 5. Plot of X-ray emission and bubble axial speed. Note the correspondence of bubble launch episodes and X-ray emission.

of a typical magnetic bubble and jet observed in the experiments is shown in Figure 4.

During the first 200 ns (times are given from the start of the current pulse), the initial ablation phase of the foil produces ambient plasma extending for a few millimeters above the foil. Electron density data obtained through laser interferometry show an exponentially decreasing axial profile, indicative of thermal expansion. Simulations indicate that there is little magnetic field embedded in this high-beta plasma. After $\sim 230$ ns, the axial component of the magnetic pressure is large enough to break through the foil, effectively creating a gap ($\sim$ 1 mm) between the anode and the left-over foil. The magnetic field then acts as a piston accelerating and sweeping the ambient plasma into a shocked layer which confines and delineates the bubble. At the same time, a current-carrying jet forms on the axis of the bubble via the "pinching" effect of the toroidal magnetic field.

The dynamics of this first bubble and jet are essentially the same as those observed in our experiments using radial wire arrays (Lebedev et al. 2005). However in the work presented here we are able to produce and observe for the first time a periodic activity of magnetic bubbles and jet formation. The main difference in the present experiments is the radial density distribution of the plasma mass source. While for the radial wire arrays it is constant, for the foil the density distribution increases linearly with the radius. Therefore, the initial gap produced by the magnetic field can be more easily refilled by the readily available plasma expanding from the remaining foil. In addition, plasma can also expand from the radiatively heated central electrode. Closure of the gap essentially halts the flux of electromagnetic energy (Poynting flux) into the bubble. The currents can once again flow across the closed gap at the base of the magnetic cavity and the initial magnetic field configuration is thus once again re-established until a new bubble is produced. Inside the already formed magnetic cavity, the magnetic Reynolds number is high and each bubble continues expanding, carrying its own trapped magnetic flux. A tight correlation exists between the observed X-ray emission and the formation of each new bubble/jet system. Figure 5 shows both the filtered X-ray emission and the axial position of the top of three magnetic bubbles measured from time-resolved self-emission images obtained during one single experiment. The extrapolated linear fit to the spatial data matches very well the start of the emission and is consistent with the X-ray bursts being associated with the formation of the magnetic bubble and jet, and the ensuing compressional heating of the plasma. The fast rising ($\sim$ 5 ns) part and peak of the emission are related to the maximum compression of the jet.

Time-resolved images of XUV self-emission spanning a period of $\sim 120$ ns are shown in Figure 6 and are representative of the evolution of the system. The first image (Figure 6a) at 286 ns corresponds to part of the data presented in Figure 5 and shows the time just after the merging of the first two magnetic bubbles. The newly formed (3rd) bubble can be clearly seen on the interior of the larger, merged cavities. The subsequent three images (Figure 3b-d) show the times 346 ns, 376 ns and 406 ns, respectively, and were taken during a single experiment. It shows the presence of multiple cavities and jets over length scales spanning over an order of magnitude. In general, the current-carrying jet is confined on the axis of the cavitiy by the toroidal magnetic field and it is in a configuration prone to current-driven (CD) instabilities, the most disruptive being the "sausage" or "pinch" and "kink" modes. The characteristic growth time is of the order of the Alfven crossing

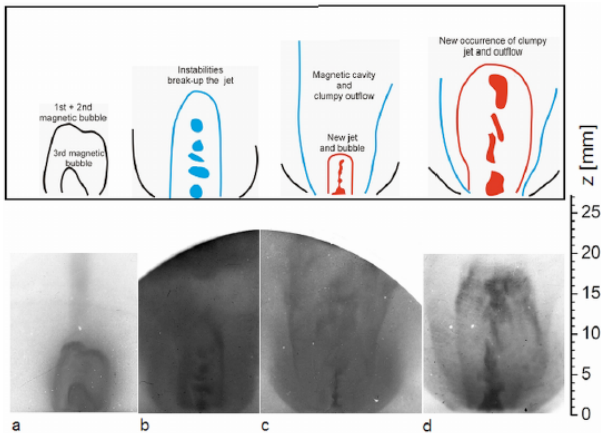


Fig. 6. Time-series of filtered XUV emission images. The timings on the images are: (a) 286 ns, (b) 346 ns, (c) 376 ns, (d) 406 ns. Panels b, c and d from the same experimental shot. The schematic cartoon above the XUV emission images serve to guide the eye in identifying the various features described in the main text.

time. It is important to note that the whole evolution of the instabilities, well into the non-linear regime, can be followed throughout the episodic jet ejections. Indeed, a fundamental insight provided by our laboratory studies is that while the instabilities ultimately lead to the break-up of the jet, they do not destroy the outflow altogether, leading instead to a heterogeneous and clumpy outflow. The magnetic field is also substantially modified by the instabilities, with the kink mode in particular leading to the generation of a poloidal magnetic flux out of the initial toroidal flux and to the tangling of the field inside the magnetic cavity. Combined with the periodic formation and burst of bubbles, the flow is effectively injected into a long lasting and well collimated channel, which is made up of multiple, nested cavities. Such morphology is shown in Figure 6, where a jet surrounded by a bow shock is clearly visible embedded inside a larger cavity. Recall, however, that the bow-shaped shock envelope is driven by the magnetic field and not hydrodynamically by the jet.

As has been discussed in detail by a variety of authors (Lebedev et al. 2005) laboratory experiments have bearing on astrophysical problems when key dimensionless parameters for both systems are in appropriate regimes. The experiments presented above considerably extend the range of the dimensionless parameters that are obtained in laboratory explorations of jet/outflows. The typical length scale of the evolved laboratory system is $L \sim 3$ cm, which combined with characteristic velocity, temperature and density in the cavity $V \sim 100$ km s$^{-1}$, $T \sim 50$ eV and $\rho \sim 10^{-5}$ g cm$^{-3}$ respectively, gives $Re \sim 5 \times 10^5$, $Re_M \sim 500$ and $Pe \sim 50$. In addition, the sonic and alfvenic Mach (ratio of the flow speed to the Alfven speed) numbers in the jet are $M \sim M_A \sim 5 - 10$, both of which are well matched with those expected in astrophysical flows. The ratio of thermal to magnetic pressure (plasma-$\beta$) can vary considerably between the dense jet and the magnetic cavity both spatially and temporally. Initially, the magnetic bubble is magnetically dominated, with $\beta \ll 1$; however in the evolved cavity, after the onset of instabilities we find $0.1 < \beta \sim 1$, while for the jet/outflow, we find $\beta \sim 1$. We also note that the plasma is highly collisional and cools effectively via radiative losses.

## 2. CONCLUSIONS

Taken together, our 3D simulations of a new "collimated clumps" scenario for protostellar jets and our laboratory experiments of such jets offer a fundamentally different paradigm for understanding jet origins and dynamics. Jet heterogeneity is seen as being intrinsic in a way that links the jet morphology on "meso-scales" to the processes (such as instabilities) occurring on "micro-scales" near the central engine.

While the pulsed-jet model has been successful at interpreting some aspects of jets, it may be misleading if used too generally. In particular, the assumption of sinusoidal pulsations can limit the interpretation of HH object observations. In our simulations, which had no sinusoidal variation in time, we nonetheless were able to recover (erroneous) sinusoidal behavior using an analysis similar to that which has been carried out on observations. While one part of this behavior (the mean velocity $v_{j,0}$) fit the initial conditions well, the derivation of pulsation periods leads to the false conclusion that the structures in the beam arose due to periodic ejection behavior. We therefore conclude that care should be taken when attributing observations of apparent sinusoidal velocity variability in protostellar jets to corresponding sinusoidal behavior of a central engine.

In contrast to pulsed-jet models, our model offers two attractive features: first, a natural mechanism (knot-knot interactions) helps explain small-scale features along the jet axis. The idea that knots or bow shocks in HH objects are evolving clumpy structures has been discussed before in the context of observations with ongoing HST observations giving continued support to this idea, e.g. (Hartigan et al. 2005). The interaction of distinct sub-radial knots

with each other and with an overall bow shock offers a simple explanation for such evolution. The second feature the model offers is the presence of unique observational characteristics in the form of forward- and reverse-facing bow shocks and spur shocks at the edges of the jet beam. Our scenario provides a simple mechanism for the formation of sub-radial, non-axisymetric features via multiple dense clumps which have a nonzero velocity dispersion. The ease with which non-axisymmetric features like spur shocks (Heathcote et al. 1996) develops in our models is attractive.

What would be the origin of the entrained clumps? The issues of the stability of jets particularly at "micro-scale" regions near the launch region remains unresolved. Our experiments address this issue, demonstrating that magnetized jet beams in the lab break up into a sequence of quasi-periodic knots due to the kink (m=0) or sausage (m=1) instabilities . These knots may be displaced slightly to the side of the nominal jet axis and may propagate with varying velocities. This results in morphologies qualitatively reminiscent of HH-jet beams. It seems plausible that a similar process could occur in the astrophysical context, beginning with a smooth beam near the central engine which then becomes disrupted owing to the kink or sausage instabilities on intermediate scales. This would result in a series of knots which continue to evolve as they propagate away from the central engine. Such a scenario would also explain the observed velocity differences between knots, attributable to the particulars of each knot's formation. Thus, we conclude that the interpretation of jets as heterogenous systems of knots has attractive features that can relate the dynamics of the jet launching to processes/features observed at larger scales.

Support for this work was in part provided by NASA through awards issued by JPL/Caltech through Spitzer program 20269 and 051080-001, the National Science Foundation through grants AST-0507519 as well as the Space Telescope Science Institute through grants HST-AR-10972, HST-AR-11250, HST-AR-11252 to. We also thank the University of Rochester Laboratory for Laser Energetics and funds received through the DOE Cooperative Agreement No. DE-FC03-02NA00057.

## REFERENCES

Bally, J., Heathcote, S., Reipurth, B., Morse, J., Hartigan, P., & Schwartz, R. 2002, AJ, 123, 2627
Biro, S., & Raga, A. C. 1994, ApJ, 434, 221
Ciardi, A., et al. 2007, Phys. Plasmas, 14, 056501
Cunningham, A. J., Frank, A., Varniere, P., Mitran, S., & Jones, T. W. 2009, ApJS, 182, 519
de Gouveia Dal Pino, E. M. 1999, ApJ, 526, 862
de Gouveia dal Pino, E. M., & Cerqueira, A. H. 1999, Ap&SS, 240, 211
Hartigan, P., Heathcote, S., Morse, J. A., Reipurth, B., & Bally, J. 2005, AJ, 130, 2197
Hartigan, P., Frank, A., Varniére, P., & Blackman, E. G. 2007, ApJ, 661, 910
Heathcote, S., Morse, J. A., Hartigan, P., Reipurth, B., Schwartz, R. D., Bally, J., & Stone, J. M. 1996, AJ, 112, 1141
Lebedev, S. V., et al. 2004, ApJ, 616, 988
Lebedev, S. V., et al. 2005, MNRAS, 361, 97
Masciadri, E., Velázquez, P. F., Raga, A. C., Cantó, J., & Noriega-Crespo, A. 2002, ApJ, 573, 260
Norman, C., & Silk, J. 1979, ApJ, 228, 197
Raga, A. C., Binette, L., Canto, J., & Calvet, N. 1990, ApJ, 364, 601
Raga, A. C., & Biro, S. 1993, MNRAS, 264, 758
Raga, A. C., & Noriega-Crespo, A. 1992, RevMexAA, 24, 9
Raga, A. C., Riera, A., Masciadri, E., Beck, T., Böhm, K. H., & Binette, L. 2004, AJ, 127, 1081
Raga, A. C., Velázquez, P. F., Cantó, J., & Masciadri, E. 2002, A&A, 395, 647
Rubini, F., Lorusso, S., Del Zanna, L., & Bacciotti, F. 2007, A&A, 472, 855
Yirak, K., Frank, A., Cunningham, A., & Mitran, S. 2008, ApJ, 672, 996
_____. 2009, ApJ, 695, 999